

Role of Heme Vinyl Groups in Cytochrome b_5 Electron Transfer

Lorne S. Reid,¹ Anthony R. Lim, and A. Grant Mauk*

Contribution from the Department of Biochemistry, University of British Columbia, Vancouver, British Columbia V6T 1W5, Canada. Received April 4, 1986

Abstract: The involvement of the heme vinyl groups in the mechanism by which cytochrome b_5 changes oxidation state has been investigated by analysis of the oxidation-reduction equilibrium and Fe(EDTA)²⁻ reduction kinetics of deuteroheme-substituted cytochrome b_5 . The reduction potential of the modified protein was determined with an optically transparent thin-layer electrode to be -44 (5) mV vs. NHE with $\Delta H^\circ = -13.9$ (1) kcal/mol and $\Delta S^\circ = -34.6$ (3) eu [pH 7.0 (phosphate), $I = 0.1$ M, 25 °C]. The ionic strength dependence of the reduction potential was determined, and the results fitted to a form of the Debye-Hückel equation were found to be consistent with an apparent electrostatic charge on the protein of -6.5 [pH 7 (phosphate), 25 °C]. The rate of deuteroheme-substituted cytochrome b_5 reduction by Fe(EDTA)²⁻ is 34 (2) M⁻¹ s⁻¹ [pH 7.0 (phosphate), $I = 0.1$ M] with $\Delta H^\ddagger = 6.8$ (1) kcal/mol and $\Delta S^\ddagger = -26.5$ (4) eu [pH 7.0 (phosphate), $I = 0.5$ M]. The pH dependence of this reaction was studied between pH 6 and 8.5 and found to be approximately 20% attributable to the effect of pH on the reduction potentials of the reactants, which is similar to the behavior of the native protein. The ionic strength dependence of this rate was determined and found to be consistent with an apparent electrostatic charge for the protein in this reaction of -14.5, a result essentially identical with that reported previously for the native protein. From these results, we conclude that the principal effect of the heme vinyl groups on cytochrome b_5 function arises from their influence on the reduction potential of the protein. This observation combined with examination of the three-dimensional structures of several heme proteins and with related measurements reported for deuteroheme-substituted myoglobin leads us to conclude that heme proteins can affect the reduction potentials of their heme redox centers by constraining the position of the vinyl groups with respect to the plane of the heme and thereby affecting the electron-withdrawing ability of the vinyls. By forcing the vinyl substituents into the plane of the heme prosthetic group, their electron-withdrawing ability is enhanced, and the reduction potential of the heme center is increased. This interpretation is in agreement with the recent NMR analyses of cytochrome c peroxidase (Satterlee, J. D.; Erman, J. E. *J. Biol. Chem.* **1983**, 258, 1050) and model heme compounds (Balke, V. L.; Walker, F. A.; West, J. T. *J. Am. Chem. Soc.* **1985**, 107, 1226).

Although the roles of heme substituent groups in determining the functional properties of myoglobin and hemoglobin have been studied extensively,² their involvement in cytochrome function has not been as thoroughly considered because the most experimentally accessible cytochrome, cytochrome c , has a covalently bound prosthetic group and, therefore, is not amenable to heme substitution experiments. Cytochrome b_5 , however, has a noncovalently bound heme group and, as its three-dimensional structure is known to high resolution,³ provides a convenient means by which the contribution of heme substituents to cytochrome function may be assessed. Previous studies from our laboratory have evaluated the functional properties of native cytochrome b_5 ⁴ and have demonstrated roles for the heme propionate groups.⁵ The present report considers the role of the heme vinyl groups by analyzing the oxidation-reduction equilibrium and Fe(EDTA)²⁻ reduction kinetics of deuteroheme-substituted cytochrome b_5 , a form of the protein in which the heme vinyl groups have been replaced with protons.

Experimental Section

Trypsin-solubilized cytochrome b_5 was isolated and purified from bovine liver microsomes and its apoprotein prepared as described previously.^{4a,5} Ferrideuteroporphyrin IX (Porphyrin Products, Logan, UT, lot 319) was dissolved in a minimal volume of 0.1 M NaOH, centrifuged to remove any insoluble material, and diluted with water to give a 1 mM stock solution ($A_{383} = 55 \pm 5$ mM⁻¹ cm⁻¹). The deuteroheme

was added to cold apocytochrome b_5 (30-100 mg) at a 1:1 molar ratio, and the absorbance at 402 nm was monitored until no further increase was detectable. In general, reconstitution was complete in 1 h. The protein solution was adjusted to pH 7.2 and concentrated to a volume of 1 mL by ultrafiltration (Amicon YM-5 membrane). The reconstituted protein was applied to a 70 × 2.5-cm column of Sephadex G-75 superfine (Pharmacia) that was equilibrated with 20 mM sodium phosphate buffer (pH 7.2 at 4 °C), and the protein was eluted with this same buffer in the cold. A brown band of unbound heme eluted after the bright red, reconstituted cytochrome. Protein fractions with an A_{402}/A_{280} ratio ≥ 6.0 were pooled and concentrated by ultrafiltration. The deuteroheme-substituted protein was recovered with a yield of 80-85% ($A_{403} = 122000$ M⁻¹ cm⁻¹) and stored in liquid nitrogen.

Potentiometric titrations were performed with an optically transparent thin-layer electrode as described previously^{4b} with a saturated calomel reference electrode and with Ru(NH₃)₆Cl₃⁷ as mediator. The resulting midpoint potentials were converted to the hydrogen scale.⁸ Kinetics measurements were made with a modified Durum-Gibson stopped-flow spectrophotometer (Dionex, Sunnyvale, CA) interfaced to a computer.^{4a} The data reduction techniques employed have been described.^{4,5}

Results

The electronic absorption spectra of reduced and oxidized deuteroheme-substituted cytochrome b_5 were found to be similar to those reported previously by Ozols and Strittmatter.⁶ On the basis of the molar absorptivity reported by these authors for the Soret band of the oxidized derivative, the maxima (nm) and millimolar absorptivities found for the reduced protein in the present work are as follows: 409.5 (156.8), 516.5 (13.3), and 543.5 (19.3). Isobestic points between the oxidized and reduced forms of the protein were observed at the following wavelengths: 345, 406, 429, 501, 525, 536, and 552 nm.

Examples of these spectra are provided in Figure 1, which depicts a family of spectra obtained during a spectroelectrochemical experiment. At pH 7.0 (phosphate), $I = 0.1$ M and 25 °C, the average midpoint reduction potential obtained from a Nernst plot (E_{app} vs. $\log ([O]/[R])$) derived from these data is

(1) Present address: Laboratory of Molecular Biology, Department of Crystallography, Birkbeck College, University of London, London, England WC1E 7HX.

(2) Asakura, T.; Lau, P. W.; Sono, M.; Adachi, K.; Smith, J. J.; McCray, J. A. *Hemoglobin and Oxygen Binding*; Ho, C., Ed.; Elsevier Biomedical: New York, 1982; p 177 and references therein.

(3) (a) Mathews, F. S.; Levine, M.; Argos, P. *J. Mol. Biol.* **1972**, 64, 449. (b) Mathews, F. S.; Argos, P.; Levine, M. *Cold Spring Harbor Symp. Quant. Biol.* **1971**, 36, 387. (c) Argos, P.; Mathews, F. S. *J. Biol. Chem.* **1975**, 250, 747. (d) Mathews, F. S. *Biochim. Biophys. Acta* **1980**, 622, 375.

(4) (a) Reid, L. S.; Mauk, A. G. *J. Am. Chem. Soc.* **1982**, 104, 841. (b) Reid, L. S.; Taniguchi, V. T.; Gray, H. B.; Mauk, A. G. *J. Am. Chem. Soc.* **1982**, 104, 7516.

(5) Reid, L. S.; Mauk, M. R.; Mauk, A. G. *J. Am. Chem. Soc.* **1984**, 106, 2182.

(6) Ozols, J.; Strittmatter, P. *J. Biol. Chem.* **1964**, 239, 1018.

(7) Recrystallized from commercial material (Alfa) as described in Pladzewicz, J. R.; Meyer, T. J.; Broomhead, J. A.; Taube, H. *Inorg. Chem.* **1973**, 12, 639.

(8) Dutton, P. L. *Methods Enzymol.* **1978**, 54, 411.

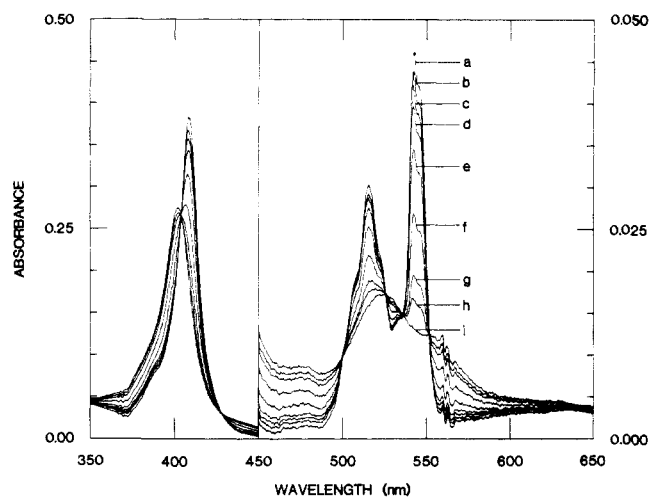


Figure 1. Representative family of thin-layer spectra of deuteroheme-substituted cytochrome b_5 at various values of applied potential, E_{app} (mV vs. NHE). Deuteroheme-substituted cytochrome b_5 (120 μ M), $Ru(NH_3)_6Cl_3$ (12 μ M), 20 $^\circ$ C, pH 7.0 (phosphate), $I = 0.1$ M: (a) -203.9, (b) -93.9, (c) -73.9, (d) -53.9, (e) -33.9, (f) -13.9, (g) 6.1, (h) 26.1, (i) 246.1. The midpoint potential calculated from a Nernst plot of these data is -38.0 (3) mV, and the Nernst slope is 58.2 mV.

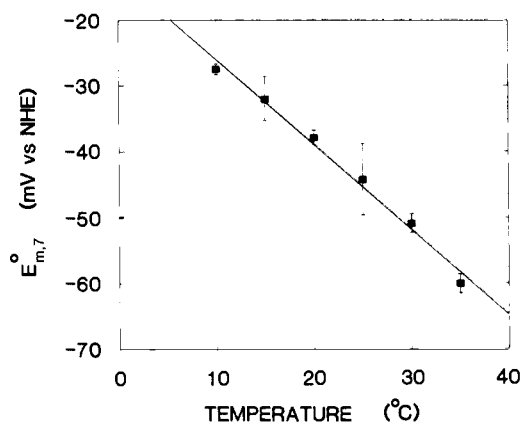


Figure 2. Temperature dependence of the deuteroheme-substituted cytochrome b_5 midpoint reduction potential [pH 7.0 (phosphate) $I = 0.1$ M]. The solid line is a weighted linear least-squares fit to the data.

-44 (5) mV with a slope of 58.9 (2) mV. The thermodynamic parameters for this equilibrium were determined⁹ from the data shown in Figure 2 to be $\Delta H^\circ = -13.9$ (1) kcal/mol and $\Delta S^\circ = -34.6$ (3) eu [pH 7.0 (phosphate) $I = 0.1$ M].

The variation in the reduction potential of deuteroheme-substituted cytochrome b_5 with pH is shown in Figure 3. As described in detail before (ref 4b and 5 and references therein), data of this type can be analyzed most simply in terms of a redox-linked functional group the pK of which is dependent on the oxidation state of the protein as described by eq 1. The solid line shown

$$E_m^\circ = E + \frac{RT}{nF} \ln \frac{K_{red} + [H^+]}{K_{ox} + [H^+]} \quad (1)$$

in Figure 3 represents a nonlinear least-squares fit of the data to this equation and is consistent with a pK for this redox-linked ionizable group of 5.9 in the oxidized state and 6.2 in the reduced state with $E = -13$ mV.

The ionic strength dependence of the midpoint reduction potential (Figure 4) may be analyzed in terms of the Debye-Hückel relationship as developed by Schejter and co-workers (eq 2).¹⁰ In

$$E^\circ_{obsd} = E^\circ - \frac{RT}{F} A(q_{ox}^2 - q_{red}^2)f(\mu) \quad (2)$$

(9) Taniguchi, V. T.; Sailasuta-Scott, N.; Anson, F. C.; Gray, H. B. *Pure Appl. Chem.* **1980**, *52*, 2275.

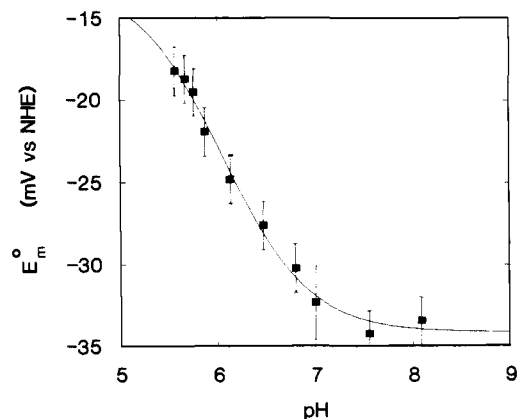


Figure 3. pH dependence of the deuteroheme-substituted cytochrome b_5 midpoint reduction potential [$I = 0.1$ M (phosphate), 25 $^\circ$ C]. The solid line is the theoretical fit of the data described in the text.

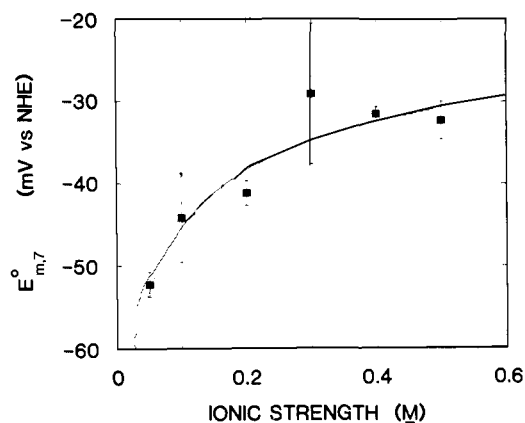


Figure 4. Variation of the deuteroheme-substituted cytochrome b_5 midpoint reduction potential with ionic strength [pH 7.0 (phosphate), 25 $^\circ$ C]. The solid line is the theoretical fit of the data described in the text.

this equation, E°_{obsd} is the reduction potential at a given ionic strength, E° is the reduction potential at an ionic strength of zero (the standard reduction potential), A is the Debye-Hückel constant (0.5115), and q_{ox} is the net electrostatic charge of the oxidized protein ($q_{red} = q_{ox} - 1$). The solid line in Figure 4 represents the nonlinear least-squares fit of the data to eq 2 where $f(\mu) = \mu^{1/2}/(1 + R\mu^{1/2})$,¹¹ and R is the radius of the protein (\AA).¹² The apparent electrostatic charge on deuteroheme-substituted cytochrome b_5 estimated from this analysis is -6.5.

Reduction of ferrideuteroheme-substituted cytochrome b_5 by $Fe(EDTA)^{2-}$ under pseudo-first-order conditions was first order for at least 85–90% of the reaction at reductant concentrations greater than 6 mM (average cytochrome b_5 concentration = 4 μ M). At lower reductant concentrations, the reaction did not proceed to completion, and the rate constant for the forward reaction was extracted by a nonlinear regression fit of the data to the following equation¹³

$$f(t) = \frac{\Delta A_{obsd}}{K_{eq}} \left[(K_{eq} + 1) \left(\frac{[(K_{eq} + 1) + \exp(k_2Qt)]}{[1 + (K_{eq} + 1) \exp(k_2Qt)]} - 1 \right) \right] \quad (3)$$

(10) Schejter, A.; Aviram, I.; Goldkorn, T. *Electron Transport and Oxygen Utilization*; Ho, C., Ed.; Elsevier Biomedical: New York, 1980; p 95.

(11) Several forms of $f(\mu)$ have been suggested (see: George, P.; Hanania, G. I. H. *Biochem. J.* **1952**, *52*, 517. Beetlestone, J. G.; Irvine, D. H. *Proc. R. Soc. London, Ser. A* **1964**, *277*, 401). Our previous work^{4b} identified this form of the function as one which provides reasonable numerical results for data of this type.

(12) The calculation of 15.2 \AA was determined as described previously.^{4b}

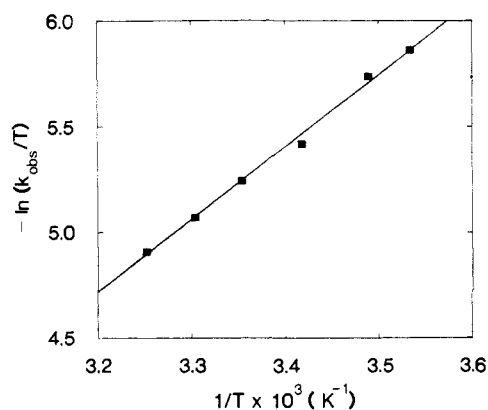


Figure 5. Eyring plot of the rate data for the reduction of deuterioheme-substituted cytochrome *b*₅ by Fe(EDTA)²⁻ [pH 7.0 (phosphate), *I* = 0.5 M]. [Fe(EDTA)²⁻] = 1.5 × 10⁻² M. Error bars are smaller than the dimensions of the symbols.

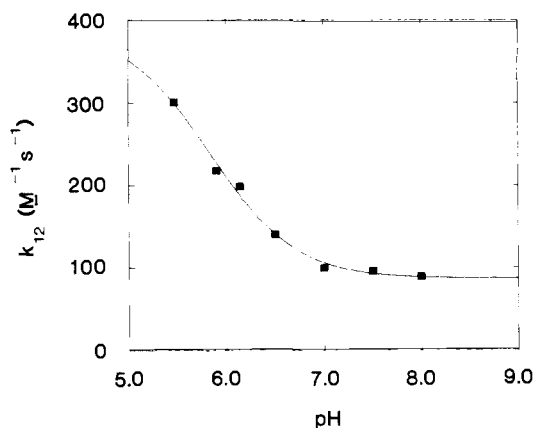


Figure 6. Dependence of the second-order rate constant for the reduction of deuterioheme-substituted cytochrome *b*₅ by Fe(EDTA)²⁻ on pH [*I* = 0.5 M (phosphate), 25 °C]. The solid line is the theoretical fit of the data described in the text. Error bars are smaller than the dimensions of the symbols.

where $Q = 1 + 2/K_{\text{eq}}$, ΔA_{obsd} is the observed change in absorbance at time t , $K_{\text{eq}} = k_2/k_{-2}$, k_2 is the forward rate constant for reduction, and k_{-2} is the rate constant for the reverse reaction. The linearity and zero intercept of the plot of first-order rate constants calculated from the fit to this relationship at several reductant concentrations demonstrate that this analysis is consistent with the experimental data. The second-order rate constant for the reduction of ferrideuterioheme-substituted cytochrome *b*₅ by Fe(EDTA)²⁻ was found to be 34 (2) M⁻¹ s⁻¹ [pH 7.0 (phosphate) *I* = 0.1 M] with $\Delta H^\ddagger = 6.8$ (1) kcal/mol and $\Delta S^\ddagger = -26.5$ (4) eu [pH 7.0 (phosphate) *I* = 0.5 M] (Figure 5).

The pH dependence of this reaction is shown in Figure 6. Previously, data of this type have been analyzed by assuming the presence of an ionizable functional group on the protein, the protonation status of which affects the rate of reaction,^{4a,5,13} and the solid line shown in Figure 6 is the nonlinear least-squares fit of our data to the equation normally used to analyze results of this sort.⁵ The resulting fit yields a rate constant for reduction of the protonated form of the protein (k_a) of 390 M⁻¹ s⁻¹ and for reduction of the deprotonated form (k_b) of 87 M⁻¹ s⁻¹ with the pK_a for interconversion of the two forms of 5.84.

In the past, this type of analysis has necessarily ignored the effect of pH on the reduction potentials of the reactants and the resulting effect on the rate of reaction because midpoint reduction potentials for both reactants as a function of pH have not been

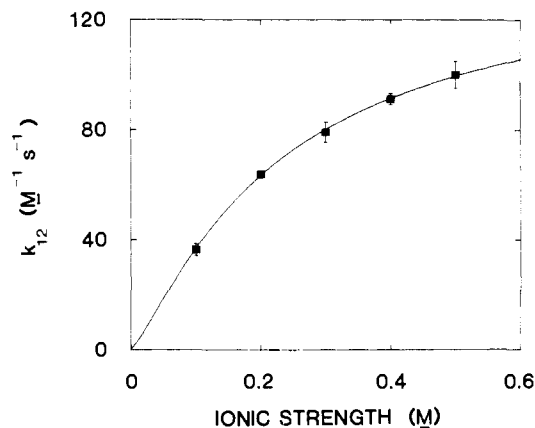


Figure 7. Ionic strength dependence of the second-order rate constant for the reduction of deuterioheme-substituted cytochrome *b*₅ by Fe(EDTA)²⁻ [pH 7.0 (phosphate), 25 °C]. The solid line is the theoretical fit of the data described in the text. The error bars are smaller than the dimensions of the symbols.

available. Recently, however, the variation in the reduction potential of the Fe(EDTA)^{2-/•} redox couple with pH has been determined.¹³ These data now permit us to correct the second-order rate constants determined at each pH for the effect of pH on the driving force of the reaction. Equation 4 can be derived from Marcus theory¹⁴ for this purpose for data obtained at 25 °C

$$k_{12}^{\text{adj}} = k_{12} \exp[19.48(\Delta E)] \quad (4)$$

In this equation, k_{12}^{adj} is the rate constant calculated for a thermodynamic driving force of zero, k_{12} is the observed second-order rate constant, and ΔE is the difference between the reduction potentials of the reactants (in V). Substitution of the rate constants from Figure 6 into this relationship along with the appropriate values for the reduction potentials of the reactants demonstrates that approximately 20% of the change in k_{12} with pH arises from the pH dependence of the reactant potentials.

The ionic strength dependence of deuterioheme-substituted cytochrome *b*₅ reduction by Fe(EDTA)²⁻ is illustrated in Figure 7. The solid line is a nonlinear least-squares fit of the data to the Wherland–Gray equation¹⁵ and is consistent with an apparent electrostatic charge on the protein of -14.5 (assumed protein radius = 17 Å) or -12.2 (assumed protein radius = 15.2 Å).¹² By using the latter value, we calculate the electrostatics-corrected self-exchange rate for the protein based on this reaction,¹⁵ k_{11}^{corr} , to be 2.2 M⁻¹ s⁻¹ and R_p ¹⁶ to be 4.9 Å. The similarly calculated values for the native cytochrome are 1.3 M⁻¹ s⁻¹ and 4.8 Å, respectively.¹³

Discussion

The principal effect of replacing the heme vinyl groups with protons on the functional properties of cytochrome *b*₅ is a lowering of the reduction potential by approximately 49 mV. This finding is consistent with the notion that the electron-withdrawing properties of the heme vinyl groups function to destabilize the oxidized form of the protein relative to the reduced form and thereby make the Fe(II)/Fe(III) reduction potential more positive. A more refined interpretation can be developed on the basis of two previous reports. In the first of these, NMR analysis of cytochrome *c* peroxidase as a function of pH led Satterlee and Erman to conclude that the orientation of one of the heme vinyl groups varies with pH and that this variation may affect the

(14) Marcus, R. A. *Ann. Rev. Phys. Chem.* **1964**, *15*, 155.

(15) Wherland, S.; Gray, H. B. *Proc. Natl. Acad. Sci. U.S.A.* **1976**, *79*, 2950. For these calculations, the following values were used (sodium phosphate (pH 7.0) *I* = 0.5 M). (a) Native cytochrome *b*₅: $k_{12} = 281$ M⁻¹ s⁻¹, $E_{m,7}^\circ = 16$ mV, $Z_1/Z'_1 = -13.5/-14.5$. (b) Deuterioheme cytochrome *b*₅: $k_{12} = 106$ M⁻¹ s⁻¹, $E_{m,7}^\circ = -31$ mV, $Z_1/Z'_1 = -12.2/-13.2$. In each case, the reduction potential of the Fe(EDTA)^{2-/•} couple was taken from a fit to these data.¹³ as 92 mV.

(16) Mauk, A. G.; Scott, R. A.; Gray, H. B. *J. Am. Chem. Soc.* **1980**, *102*, 4360.

(13) Reid, L. S. Ph.D. Dissertation, University of British Columbia, 1984. The reduction potentials observed for the Fe(EDTA)^{2-/•} couple are as follows [sodium phosphate, *I* = 0.5 M (0.25 M from NaI), 25 °C] (mV vs. NHE): pH 5.5, 115.7 (7); pH 6.0, 104.1 (7); pH 6.5, 98.4 (5); pH 7.0, 95 (1); pH 7.5, 86.8 (9); pH 8.0, 86.9 (8).

Table I. Orientation of Vinyl Groups in Heme Proteins as Determined from X-ray Diffraction Data^a

protein ^b	source	form	file ^c	dihedral angle (deg) ^d	
				2-vinyl	4-vinyl
cytochrome <i>b</i> ₅ (2.0)	beef liver	Fe ^{III}	2B5C	12 ± 9	1 ± 6
cytochrome <i>b</i> ₅₆₂ (2.5)	<i>E. coli</i>	Fe ^{III}	156B	5 ± 8	17 ± 7
Myoglobin (2.0)	sperm whale	Fe ^{III} H ₂ O	2MBN	30 ± 12	30 ± 12
myoglobin (1.4)	sperm whale	Fe ^{II} (deoxy)	1MBD	35 ± 10	1 ± 6
myoglobin (2.0)	sperm whale	Fe ^{II} (deoxy)	3MBN	30 ± 12	30 ± 12
leghemoglobin (2.0)	yellow lupin	Fe ^{II} (deoxy)	1LH4	26 ± 10	84 ± 10
leghemoglobin (2.0)	yellow lupin	Fe ^{III} H ₂ O	2LH2	34 ± 10	87 ± 10
leghemoglobin (2.0)	yellow lupin	Fe ^{II} (deoxy)	2LH4	32 ± 10	86 ± 10
leghemoglobin (2.0)	yellow lupin	Fe ^{III} H ₂ O	1LH2	31 ± 9	90 ± 10
erythrocrucorin (1.4)	<i>Thummi thummi</i>	Fe ^{III} H ₂ O	1ECA	40 ± 10	63 ± 10
erythrocrucorin (1.4)	<i>Thummi thummi</i>	Fe ^{II} (deoxy)	1ECD	33 ± 10	63 ± 10
hemoglobin	horse	Fe ^{II} (deoxy)	2DHB		
α chain (2.8)				34 ± 6	15 ± 7
β chain (2.8)				59 ± 9	12 ± 6
hemoglobin	human	Fe ^{II} (deoxy)	2HHB		
α chain (1.74)				50 ± 10	43 ± 10
β chain (1.74)				41 ± 12	43 ± 10
hemoglobin	human	Fe ^{II} (deoxy)	3HHB		
α chain (1.74)				45 ± 10	31 ± 9
β chain (1.74)				52 ± 10	42 ± 10
hemoglobin	horse	Fe ^{III} H ₂ O	2MHB		
α chain (2.0)				34 ± 10	56 ± 10
β chain (2.0)				50 ± 10	46 ± 10
catalase	bovine liver	Fe ^{III}	8CAT		
α chain (2.5)				3 ± 7	50 ± 9
β chain (2.5)				5 ± 11	67 ± 10
catalase (3.0)	<i>P. vitale</i>	Fe ^{III}	4CAT	0 ± 10	0 ± 11
cytochrome <i>c</i>	<i>S. cerevisiae</i>	Fe ^{III}	<i>e</i>	34 ± 10	37 ± 13
peroxidase (1.7)					
cytochrome	<i>P. putida</i>	Fe ^{III} (camphor)	<i>f</i>	18 ± 10	89 ± 9
P-450-cam (1.7)					

^aProtein coordinates were obtained from the Brookhaven Protein Data Bank²⁰ except where noted. ^bThe numbers in parentheses indicate the resolution reported for the crystallographic coordinates in Å. ^cData set designation of the Brookhaven Protein Data Bank. ^dThe uncertainties indicated for the angles arise from uncertainties in determining the planes of the associated pyrrole rings. ^eHeme coordinates obtained from Finzel, B.; Poulos, T. L.; personal communication. ^fHeme coordinates obtained from Poulos, T. L., personal communication.

activity of the enzyme by influencing its reduction potential.¹⁷ NMR studies of simpler heme proteins¹⁸ combined with extensive studies of model heme compounds have independently led Walker and co-workers to similar conclusions regarding the role of heme vinyl groups.¹⁹ In brief, both groups propose that the amino acid residues lining the heme binding pocket of a heme protein may restrict the orientation of the heme vinyl groups and thereby regulate their electron-withdrawing ability. In this way, the protein environment could modulate the heme iron reduction potential in a manner not previously appreciated.

Although three-dimensional structures have been determined for a large number of heme proteins, heme vinyl group orientations in these structures have not generally been discussed because their potential significance has been unrecognized. To assess the variation in vinyl group orientation observed in heme proteins, we have surveyed the crystallographic coordinates deposited in the Brookhaven Protein Data Bank²⁰ to produce the compilation set out in Table I. As seen in this listing, the 2-vinyl group has been found to vary from being coplanar with the adjacent pyrrole ring to being 59° out-of-plane, while the 4-vinyl group ranges from being coplanar to being orthogonal. Clearly, the apoprotein environments do appear to exert considerable influence on the heme vinyl group orientation and, by implication, their electron-withdrawing ability.

We note that a truly rigorous analysis of this type requires comparison of vinyl angles in both oxidation states of the proteins considered. At present, there are insufficient crystallographic data

available to permit such analysis. Interestingly, the three proteins for which this information is currently available demonstrate different behavior. That is, the 4-vinyl group of horse heart hemoglobin appears to move by 30–40° out of the plane of the heme on oxidation of the iron, while the vinyl groups of myoglobin and leg hemoglobin do not undergo a significant change in orientation with oxidation state. The report by Satterlee and Erman¹⁷ that the vinyl group orientation in cytochrome *c* peroxidase varies with pH, however, indicates that the present crystallographically based discussion may represent simply an initial approximation of what transpires in solution.

Myoglobin is the only other heme protein that has been studied in a manner similar to that employed in the current analysis of cytochrome *b*₅. Brunori and co-workers have reported electrochemical studies for deuteroheme-substituted myoglobin²¹ that indicate that its potential is 22 mV lower than that of the native protein. As this difference is less than the difference between the potentials of native and deuteroheme-substituted cytochrome *b*₅, the model described above would predict that the heme vinyl groups of cytochrome *b*₅ are more in the plane of the heme than are the heme vinyl groups of myoglobin. This prediction is borne out by the structural data set out in Table I. While this correlation is consistent, more data are clearly required to establish the validity of our interpretation and to estimate the magnitude of the effect that manipulation of heme vinyl group orientation might be expected to exert on heme protein reduction potentials.

Our finding that the dependence of Fe(EDTA)²⁻ reduction rate on pH is approximately 20% attributable to the influence of pH on the thermodynamic driving force of the reaction establishes that most of the effect of pH on this reaction is, in fact, kinetic in origin. In light of this finding, we have now reanalyzed the results that we reported previously for reduction of the native

(17) Satterlee, J. D.; Erman, J. E. *J. Biol. Chem.* **1983**, *258*, 1050.

(18) LaMar, G. N.; Budd, D. L.; Smith, K. M.; Langry, K. C. *J. Am. Chem. Soc.* **1980**, *102*, 1822.

(19) Balke, V. L.; Walker, F. A.; West, J. T. *J. Am. Chem. Soc.* **1985**, *107*, 1226.

(20) Bernstein, F. C.; Koetzle, T. F.; Williams, C. J. B.; Meyer, E. F., Jr.; Brice, M. D.; Rodgers, J. R.; Kennard, O.; Shimanouchi, T.; Tasumi, M. *J. Mol. Biol.* **1977**, *97*, 1977.

(21) Brunori, M.; Saggese, U.; Rotilio, G. C.; Antonini, E.; Wyman, J. *Biochemistry* **1971**, *10*, 1604.

protein by $\text{Fe}(\text{EDTA})^{2-4a}$ with eq 4 and find that about 30% of the pH dependence of this reaction results from the pH dependence of the thermodynamic driving force.

The similarity of the results reported here for the ionic strength dependences of the reduction potential and $\text{Fe}(\text{EDTA})^{2-}$ reduction kinetics with those previously observed for the native protein^{4a} is not altogether surprising insofar as the heme vinyl groups are located in the interior of the heme binding pocket of the cytochrome. In this location they would not be expected to contribute appreciably to the apparent surface properties of the protein. In combination, the results obtained from both the ionic strength dependence analysis, the pH dependence analysis, and the Marcus calculations for the $\text{Fe}(\text{EDTA})^{2-}$ reduction kinetics of the native and deuterioheme-substituted cytochrome establish the identity of reaction mechanism that each employs in its reaction with this

and presumably with other small molecule oxidation–reduction reagents.

Acknowledgment. We thank Dr. Bernard Santarsiero for assistance in the use of the software employed in calculation of the angles reported in Table I and for helpful discussions. We also thank Drs. Thomas L. Poulos and Barry Finzel for communicating the coordinates of the heme groups in cytochrome P-450-cam and in the refined structure of cytochrome *c* peroxidase. This research was supported by an operating Grant (MT-7182) from the Medical Research Council of Canada.

Supplementary Material Available: Listing of reduction potentials, Nernst slopes, and observed first-order rate constants (3 pages). Ordering information is given on any current masthead page.

Magnetic Exchange Interactions in Nitroxyl Biradicals Bridged by Metal–Metal Bonded Complexes: Structural, Magnetochemical, and Electronic Spectral Characterization of Tetrakis(perfluorocarboxylato)dimetal(II) Complexes of Rhodium and Molybdenum Containing Axially Coordinated Nitroxyl Radicals

Timothy R. Felthouse,^{*1a} Teng-Yuan Dong,^{1b} David N. Hendrickson,^{*1b} Huey-Sheng Shieh,^{1a} and Michael R. Thompson^{1a}

Contribution from the School of Chemical Sciences, University of Illinois, Urbana, Illinois 61801, and the Central Research Laboratories, Monsanto Company, St. Louis, Missouri 63167. Received June 12, 1986

Abstract: A series of oxygen-bonded nitroxyl biradicals bridged by $\text{M}_2(\text{O}_2\text{CR})_4$ complexes has been prepared in order to gauge the ability of the metal–metal bonded $\text{M}_2(\text{O}_2\text{C})_4$ cores to propagate a magnetic exchange interaction. The compounds have the general formula $\text{M}_2(\text{O}_2\text{CR})_4(\text{Tempo})_2$, where $\text{M} = \text{Rh}$, $\text{R} = \text{CF}_3$ (**1**); $\text{M} = \text{Rh}$, $\text{R} = \text{C}_3\text{F}_7$ (**2**); $\text{M} = \text{Rh}$, $\text{R} = \text{C}_6\text{F}_5$ (**3**); $\text{M} = \text{Mo}$, $\text{R} = \text{CF}_3$ (**4**); and Tempo is 2,2,6,6-tetramethylpiperidinyl-1-oxy. Dark green crystals of **1** and **2** were isolated from toluene solutions and the structures determined by single-crystal X-ray diffraction techniques. Crystallographic data are as follows: **1** (295 K), space group $P\bar{1}$; $a = 8.715$ (2) Å, $b = 10.765$ (3) Å, $c = 11.501$ (3) Å; $\alpha = 107.18$ (2)°, $\beta = 103.30$ (2)°, $\gamma = 107.61$ (2)°; $Z = 1$; $R_1 = 0.0355$; $R_2 = 0.0442$ for 2479 Cu $K\alpha$ data with $I > 2.33\sigma(I)$. **2** (143 K), space group $P2_1/c$; $a = 11.450$ (2) Å, $b = 16.604$ (3) Å, $c = 13.163$ (2) Å; $\beta = 90.30$ (1)°; $Z = 2$; $R_1 = 0.0614$, $R_2 = 0.0669$ for 3409 Mo $K\alpha$ data with $I > 3.00\sigma(I)$. Both structures **1** and **2** consist of typical $\text{Rh}_2(\text{O}_2\text{CR})_4$ frameworks having Rh–Rh bond lengths of 2.417 (1) and 2.431 (1) Å, respectively, while these centrosymmetric structures contain axial O-bonded Tempo ligands with Rh–O distances of 2.220 (2) and 2.234 (5) Å. Variable-temperature (~40–350 K) magnetic susceptibility data for **1–3** reveal the presence of unexpectedly strong antiferromagnetic exchange interactions in these compounds. Least-squares fitting of the χ_M data to the Bleaney–Bowers equation ($S_1 = S_2 = 1/2$ with the isotropic exchange Hamiltonian $-2J\hat{S}_1\hat{S}_2$) produces exchange parameters J of -239 , -269 , and -184 cm^{-1} for **1**, **2**, and **3**, respectively. Variable-temperature (4.2–300 K) magnetic susceptibility data were also obtained for $\text{Mo}_2(\text{O}_2\text{CCF}_3)_4(\text{Tempo})_2$ (**4**) and $\text{Rh}_2(\text{O}_2\text{CCF}_3)_4(\text{Tempo})_2$ (**5**), where Tempo is 4-hydroxy-2,2,6,6-tetramethylpiperidinyl-1-oxy. The χ_M data for **4** and **5** follow the Curie–Weiss law throughout the entire temperature range. Electronic absorption and EPR spectral data are also reported for **1–5**. Analysis of the crystal packing geometries in **1** and **2** reveals that the shortest intermolecular nitroxyl group contact distances increase from 4.7 Å in **1** to >6.1 Å in **2** largely as a consequence of the bulkier C_3F_7 groups in **2**. Closely similar singlet–triplet separations in **1** and **2** in conjunction with the lack of any observable magnetic exchange interaction in **4** and **5** suggest that the exchange interactions result from an intramolecular through bond coupling mechanism across the $\text{Rh}_2(\text{O}_2\text{C})_4$ cores despite the more than 6.8-Å separation between radical centers. A discussion is presented on the molecular orbital interactions that lead to efficient spin coupling across the singly bonded $\text{Rh}_2(\text{O}_2\text{C})_4$ framework but produce no observable exchange interaction between nitroxyl groups when bridged by the quadruply bonded $\text{Mo}_2(\text{O}_2\text{C})_4$ core. An $\text{Rh}_2\pi^*-(\text{Tempo})_p\pi^*$ back-bonding model accounts for the strong spin coupling in the $\text{Rh}_2(\text{O}_2\text{CR})_4(\text{Tempo})_2$ compounds, and it is the absence of this $\text{M}_2\pi^*$ back-bonding interaction in $\text{Mo}_2(\text{O}_2\text{CCF}_3)_4(\text{Tempo})_2$ that leads to no spin pairing in this compound. The magnitudes of the intramolecular exchange interactions in the dirhodium–biradical compounds argue against a simple distance-dependence limit function that determines the singlet–triplet separations.

Shortly after the synthesis and characterization of the first nitroxyl biradicals,^{2–5} subsequent investigations discovered a

complex relationship between the ground-state singlet–triplet separations in these biradicals and the identity, number, and